Investigation of Mechanical Properties of Al Alloy Composites through in Situ TiB_2 Reinforced

K.Venkata Sreekanth[1], Dr. T Venkateswara Rao[2]

[1]Scholar, Damisetty Bala Srinivasa Naidu Institute of Technology, A.P, India, 524201.
[2]Professor, Damisetty Bala Srinivasa Naidu Institute of Technology, A.P, India, 524201.

Abstract: The paper explores the arrangement of in situ TiB_2 through a substance response among Al, TiO_2, and B_2O_3. The thermodynamic evaluation shows the arrangement of TiB_2 through two phases, in particular, a decrease of Ti and B from their oxides followed by the development of TiB_2. 53% and 44% expansions in the yield and extreme elastic burdens of the composite supported with 15%TiB2 contrasted with its unreinforced partner have been noticed.

Keywords: Composite; Powder metallurgy; X-ray diffraction; Thermodynamics.

1. Introduction

Ceramic molecule-built up aluminum metal lattice composites (MMCs) created by in situ processes have been widely concentrated because of their possibly low fabrication cost [1-6]. In situ manufacture, a compound response prompts the development of thermodynamically stable building up clay phase(s) during the cycle. A portion of these strategies incorporates DIMOXTM, XDTM, receptive gas penetration, and high-temperature self-spreading blend (SHS). In situ MMCs can be more financially savvy and have higher mechanical strength, especially at moderately higher working gum. Saving in cost might come from the decrease or end of handling steps and the need to add building-up parts. Stage changes, recrystallization, or nucleation happening in the in situ compound interaction produce more uniform conveyance of the supporting stages in the sub-micrometer or even nanometer range bringing about better mechanical properties of the last MMCs.

Utilizing the in situ process, Al MMCs have been created utilizing different beginning material frameworks. For instance, in situ Al2O3 molecule built up Al composite has been ready by the vortex strategy where the necessary measure of TiO2 was added into the vortex framed in liquid Al at 1023 K. The decreased Ti from TiO2 is relied upon to break down into the Al soften delivering an extra reinforcing outcome [7]. TiO2 hairs have been utilized to respond with Al by response press projecting to create composite materials with the development of supporting - Al2O3 stages and fragile TiAl3 [8].

Receptive sintering has additionally been utilized to create little size TiB2-based particulate MMCs from a compacted combination of reactant powders [4]. The procedure is affordable because of modest beginning powders and somewhat low sintering temperature. Likewise, it might prompt the chance of densifying the materials with less added substances or even without added substances by any stretch of the imagination.

Al and its combinations have been picked as the framework materials chiefly because of their low liquefying point, low thickness, wide fluid temperature range, sensibly high warm conductivity, heat treatment ability, handling adaptability, accessibility, and finally their minimal expense [2,5,10]. Concerning the support, TiB2 is picked since it is especially reasonable as support for Al-based receptive sintered composites because of its high exothermic development and thermodynamic strength in Al [2,5].

In the current review, a minimal expense beginning material arrangement of Al- 4wt.%Cu/TiO2-B2O3 is utilized to manufacture in situ shaped TiB2 and Al2O3 supported Al-4wt.%Cu composites by abstaining from utilizing costly beginning powders like B or Ti or TiB2. The plausibility of obtaining TiB2 support particles in the Al/Cu grid using in situ responsive sintering is explored utilizing XRD, SEM, and EDAX. The impacts of TiB2 support with various weight proportions on the mechanical properties and microstructures of the resultant composites are additionally contemplated.

2. Experimental procedures

The nominal compositions of the MMCs fabricated in the present investigation were Al–4wt.%Cu matrix reinforced with 5, 10, and 15 wt.% in situ reactants of TiB2 particles through the following reaction:

$$10Al + 3TiO_2 + 3B_2O_3 \rightarrow 5Al_2O_3 + 3TiB_2 \text{ ------- } (1)$$

Natural Al and Cu powders were first mixed for 2 h with TiO_2 and B_2O_3 powders in a twin shell tumble blender at a rotational speed of 45 rpm. Ball processing was then done utilizing a Frisch PM/5 planetary ball processing machine working at 150 rpm for 4 h. The weight proportion of ball to powder was controlled at 10:1 for all millings. To forestall oxidation of the powders during processing, the ball processing vials were vacuumed and afterward loaded up with 99.9% unadulterated argon gas.

2.5 wt.% stearic corrosive was added as an interaction control specialist to keep away from exorbitant virus welding of the powders during processing [11].

After the processing system, the powders were cold compacted into green compacts as a circle of 35 mm width and 40 mm thick. The green compacts were sintered at various temperatures from 873 to 1023 K for 2 h in a Carbolite heater (773 K for the framework compacts). Expulsion of the preheated compacts into a 10 mm measurement bar was then done at 823 K (723 K for the lattice compacts).

The bars were solutionized at 790 K for 4 h followed by water extinguishing to guarantee the presence of a supersaturated stage. Hardness test examples of 5 mm thickness were then cut from the solutionized bars and matured at 180°C for determined time frames h. The matured specimens were then water extinguished and hardness-tried with Superficial Rockwell to concentrate on the maturing conduct of the examples as well as to decide the maturing time to top hardness.

Malleable examples of 5 mm width and 30 mm check length were machined as per the ASTM E8M-96 norm. A tractable test was done utilizing an Instron 8516 machine with the pace of stacking being controlled at 1.2%/min. A Lab XRD-6000 Shimadzu X-beam diffractometer was utilized to recognize the different stages present in the examples. Microstructures and cracked surfaces of the ductile examples were analyzed utilizing a JEOL JSM-5800LV checking electron microscope (SEM).

3. Results and discussion

Structural evolution

X-ray diffraction (**XRD**) patterns of the matrix specimen and the specimens reinforced with different amounts of TiB_2 are shown in Fig. 1. It is evident that reaction (1)takes place in all the composite specimens as indicated by the formation of TiB_2 andAl_2O_3 diffraction peaks. The intensity of both diffraction peaks increases with increasing TiO_2 and B_2O_3. In addition to the presence of TiB_2 and Al_2O_3 in the composites, Al_3Ti intermetallic compound was also detected although the amount was very low. The intermetallic compound is a by-product of the reaction between Al and Ti.

intensity

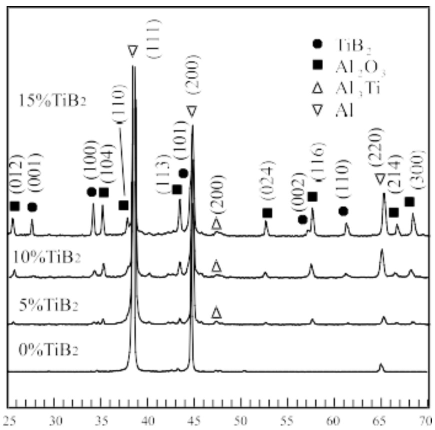

DIFFARATION ANGLE (2 $^{\theta}$)

Fig. 1. XRD patterns of the specimens with different amounts of TiB_2 reinforcements.

Table 1

Gibbs free energy of different phases at 1023 K

Phase	TiO_2	B_2O_3	Al_2B	TiB_2	Al_2O_3	Al_3Ti	Al	Ti	B
Gibbs free energy(kJ)	-1031	-1304	-217	-384	-1773	-298	-43	-46	-15

[5,6,9]. Some very weak Al_2O_3 diffraction peaks have also been detected from the matrix specimen. The formation of Al_2O_3 in the matrix Al may be associated with oxidation of the green compact during the sintering process. No TiB_2 could be discerned in the specimens that were sintered below 1023 K.

During the sintering system, a few stages, for example, TiO_2, B_2O_3, Al_2B, TiB_2, Al_3Ti, and Al_2O_3 could coincide together because of uncompleted response. Thermodynamic investigation shows that this multitude of stages is thermodynamically great. Table 1 records the Gibbs free energies of the multitude of stages at 1023 K.

From the thermodynamic information, it very well may be seen that TiB_2 can't be straightforwardly shaped from the decrease of TiO_2 and B_2O_3 since both TiO_2 and B_2O_3 have a lot of lower Gibbs free energy than that of TiB_2. Accordingly, it is recommended that the development of in situ TiB_2 be achieved through two stages. In the initial step, since the Gibbs free energy of Al_2O_3 is a lot lower than of both TiO_2 and B_2O_3, the oxygen iotas might be decreased by the removal of oxygen molecules from TiO_2 and B_2O_3 so the Ti and B particles can be liberated by the arrangement of Al_2O_3. The free Ti and B molecules have a higher likelihood to respond with the Al framework as well as respond with one another.

Accordingly, in the subsequent advance, Al_2B, Al_3Ti, and TiB_2 mixtures could be shaped. When TiB_2 is framed, it can't be disintegrated even though TiO_2 and B_2O_3 have lower Gibbs free energies. This is because Al_2O_3 has the most minimal Gibbs free energy and can't be decreased by one or the other Ti or B particles. From the thermodynamic examination, the accompanying response instruments are suggested.

In the first step, the reaction takes place as follows:

$$3TiO_2 + B_2O_3 + 6Al \rightarrow 3Al_2O_3 + 3Ti + 2B \quad \text{with } \Delta G = —832 \text{ kJ}. \qquad (2)$$

After the first reaction, TiO_2 and B_2O_3 are fully reduced. Al_2O_3 remains as the inner compound that will not participate in the further chemical reaction due to its low Gibbs free energy. In this system, only Al, Ti, and B are available to take part in further reactions. In the second step of the reaction, Ti reacts with B in the Al matrix-forming TiB_2 and Al_3Ti as follows:

$$2Ti + 2B + 3Al \rightarrow TiB_2 + Al_3Ti \text{ with } \Delta G = —431 \text{ kJ} \quad (3)$$

Fig. 2(a) provides a general view of the microstructure of the sample reinforced with 15% of TiB_2. The more detailed view is shown in Fig. 2(b). Two types of structures can be identified. The first type is the rectangularly shaped particles. From EDAX scans, this intermetallic compound was found to consist of Al and Ti. From earlier research works conducted [2,3,5–8], this intermetallic compound could be Al_3Ti has been confirmed using XRD diffraction spectrum.

a

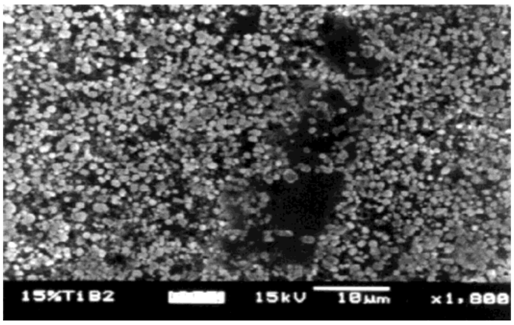

Fig. 2. Microstructures of the specimen reinforced with 15% TiB_2.

The typical TiB_2 with the unique hexagonal shape [9] can secondly be seen in Fig.2(b). Parts of the TiB_2 particles have been obscured or incorporated by the Al matrix material. A similar phenomenon has also been observed by Feng and Froyen [9]. Some parts of the TiB_2 particles at the vicinity of the Al_3Ti particles were obscured as well, indicating the possible effect of Al_3Ti engulfment within the vicinity of the Al_3Ti layer as well as the effect of matrix incorporating into the lattice of TiB_2.

From the perception that the TiB2 support particles have been mostly obscured by the grid, an end may be drawn that holding between the reinforcement particles and the Al lattice is great. The justification for the great interfacial holding maybe because of the way that in situ arrangement of particles inside the framework forestalls oxidation of the surfaces of the particles and further develops wetting conditions. As burdens can be moved from the grid to the support all the more real, load-bearing capacities of the material are expanded. Hence, the general mechanical properties of the composites are gotten to the next level. The size of the TiB2 particles was viewed as around 1 µm or more modest which is as per past discoveries that support particles shaped utilizing in situ handling were little, normally kept up with at a size of 1 µm or more modest [1].

4. Mechanical properties

It tends to be seen that the maturing time to top hardness diminishes as the level of support in the example increments. The example without support invested in some opportunity to arrive at top hardness when contrasted with the built-up examples, while the example with 15% TiB2 support took the briefest. The impact of sped up maturing is in this way observed in the supporting examples when contrasted with the unreinforced partner. The peculiarity shows an increment in disengagement thickness nearby the reinforcement, rushing the heterogeneous nucleation or potential development of the age-hardening accelerates.

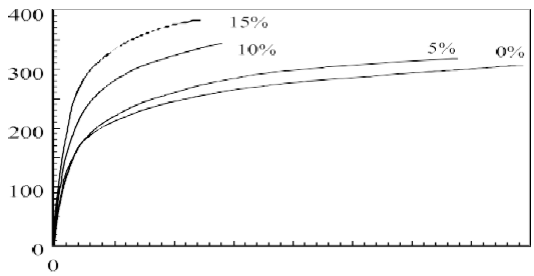

Fig. 3. Stress-strain curves for composites with different TiB_2 compositions.

The pressure strain practices of the built-up and unreinforced examples under consistent strain rate are portrayed in Fig. 4. The figure shows that the unreinforced and that built up with 5% TiB2 examples display malleable conduct while those supported with 10% and 15% TiB2 display the component of fragile conduct yet at a lot higher strength. Normal mathematical upsides of the mechanical properties are given in Table 2. A definitive rigidity (UTS), Young's modulus (E) and offset yield strength($\sigma_{0.2}$) increment essentially as the level of TiB2 support increments. For ex-adequate, upsides of UTS and E of the example supported with 15% TiB2 increment by 44% what's more 66% separately contrasted with those of the unreinforced grid amalgam. The adjustment of solidarity is accepted to be halfway because of the productive exchange of burden from the grid to the support and the great holding between them. In this way, more support particles in the examples might achieve more noteworthy expansion in strength correspondingly. Another explanation might be that the support particles can go about as obstructions to the development of the disengagements.

Table 2: Mechanical properties of the matrix and the composites

	TiB2			
	0%	5%	10%	15%
σ0.2 (MPa)	178.2	187.5	248.7	274.4
UTS (MPa)	270.0	284.1	326.3	389.5
E (GPa)	64.86	69.33	83.56	107.7
Elongation (%)	3.81	3.50	1.92	1.99

Impenetrable obstacles through which dislocations can only move by sharp changes in curvature in the dislocation line. Dislocations can only pass at stress levels much higher than those required to move dislocations through the matrix phase. Hence, an increase in reinforcement particles in the matrix manifests an improvement in the mechanical properties of the specimens as shown from the results of the present study.

From Table 2, the extension of the examples diminishes as the percentage of support increments. This reduction relates to the decline in stack up dividing because of the expansion in the level of support. The unreinforced lattice has a lot higher malleability in contrast with every one of the built-up examples. This is attributed to the lattice having the option to go through bigger plastic deformities without even a trace of weak support particles.

5. Conclusions

From the results of this study, the following conclusions can be drawn:

1. Al MMC reinforced with TiB_2 particles can be fabricated via an in situ reaction process using Al, TiO_2, and B_2O_3.
2. The formation of TiB_2 reinforcement particles was confirmed by XRD analysis and the presence of the typical hexagonal-shaped particles of TiB_2 with the size of 1 μmor less.
3. The thermodynamic assessment suggests that the formation of TiB_2 undergoes two steps, namely, the formation of Al_2O_3, and the formation of Al_2B, Al_3Ti, and TiB_2.
4. Mechanical properties obtained showed an increase in strength as the amount of TiB_2 in the specimens was increased.
5. The formation of Al_2O_3 plays an important role in the reduction of TiO_2 and B_2O_3. In addition, the presence of Al_2O_3 acts as an additional reinforcement in the composite.

References

[1] Jacobs, J. A., & Kilduff, T. F. (1997). Eng Mater Tech Prentice Hall.

[2] Gotman, I., Koczak, M. J., & Shtessel, E. (1994). Mater Sci Eng A 187, 189.

[3] Nukami, T., & Flemings, M. C. (1995). Metall Mater Trans A 26A, 1877.

[4] Zhao, H., & Cheng, Y.-B. (1999). Cera Intern 25, 353.

[5] Brinkman, H. J., Duszczyk, J., & Katgerman, L. (1997). Scripta Mater 37, 293.

[6] Feng, C. F., & Froyen, L. (1998). Scripta Mater 39, 109.

[7] Maity, P. C., Panigrahi, S. C., & Chakraborty, P. N. (1993). Scripta Metall et Mater 28, 549.

[8] Pan, J., Li, J. H., Fukunaga, H., Ning, X. G., Ye, H. Q., Yao, Z. K., & Yang, D. M. (1997). Comp Sci Tech 57, 319.

[9] Feng, C. F., & Froyen, L. (1997). Scripta Mater 36, 467.

[10] Lloyd, D. J. (1994). Int Mater Rev 39, 1.

[11] Lu, L., & Lai, M. O. (1998). Mechanical Alloying. Kluwer Academic Publishers.

[12] Janowski, G. M., & Pletka, B. J. (1995). Metall Mater Trans A 26A, 3027.